PAPER • **OPEN ACCESS**

Experimental investigation on effects of ultrasonic process parameters on the degree of impregnation of BF/PP composites

To cite this article: Yuanyuan Liu *et al* 2024 *Mater. Res. Express* **11** 045303

Materials Research Express

PAPER

Experimental investigation on effects of ultrasonic process parameters on the degree of impregnation of BF/PP composites

Yuanyuan Liu[1], **Yifei Yang**[1], **Yadong He**[1,2], **Chunling Xin**[1,2], **Feng Ren**[1,*] **and Yang Yu**[3,4,*]

[1] College of Mechanical and Electrical Engineering, Beijing University of Chemical Technology, Beijing 100029, People's Republic of China
[2] Polymer Processing Equipment Engineering Research Center, Ministry of Education, People's Republic of China
[3] Centre for Infrastructure Engineering and Safety (CIES), School of Civil and Environmental Engineeirng, The University of New South Wales, Sydney, NSW 2052, Australia
[4] Multidisciplinary Center for Infrastructure Engineering, Shenyang University of Technology, Shenyang, Liaoning 110870, People's Republic of China
[*] Authors to whom any correspondence should be addressed.

E-mail: renfeng@mail.buct.edu.cn **and** yang.yu12@unsw.edu.au

Keywords: long basalt fiber, PP, ultrasonic, melt impregnation, mechanical properties

OPEN ACCESS

RECEIVED
20 February 2024

REVISED
15 April 2024

ACCEPTED FOR PUBLICATION
22 April 2024

PUBLISHED
30 April 2024

Abstract

The properties of basalt fiber reinforced polypropylene composites (BF/PP) were improved by ultrasonic treatment of resin building pressure to assist melt impregnation. Combined with the study of ultrasonic pressure building theory, the mechanical properties of the modified composites were analyzed using the characterization of tensile, flexural and impact strengths in response to porosity and fracture rate. The effects of ultrasonic power, frequency and distance of action on resin building pressure and composite properties were investigated. The results showed that the best effect was achieved when the ultrasonic frequency was 25 kHz, the ultrasonic power was 300 W, and the action distance was 4 mm, at which time the porosity of the prepreg was reduced to 2.99%, the fracture rate was 3.36%, and the tensile, flexural, and impact strengths were 108.73 MPa, 116.81 MPa, and 51.59 KJ.m^{-2}.

1. Introduction

Fiber-reinforced resin composites are popular due to their high strength, lightweight properties, corrosion resistance, and other advantages. While thermosetting composites have their place, thermoplastic composites have promising future in aerospace, automotive, and other industries because of their ability to store prepregs for extended periods, efficient and continuous preparation, high impact toughness, and recyclability. Recently, researchers have focused on fiber-reinforced resin composites for their energy-saving, environmentally-friendly, and lightweight qualities [1–3]. Basalt fibers have unique properties, such as excellent mechanical strength, being sourced from green and pollution-free materials, corrosion resistance, sound insulation and high economy [4]. In addition, BFRP composites possess stronger creep properties, with creep fracture stresses that are 54% of their tensile strength, which allows BFRP composites to be used more fully for prestressing and cable applications than GFRP [5]. These characteristics have made basalt fiber, an inorganic material, the reinforcing fiber of choice for resin matrix composites in recent years [6].

The preparation of thermoplastic resin matrix composites by melt impregnation not only allows for precise control of the fiber content in the composite, but also has a short molding cycle, is widely used for the preparation of thermoplastic prepregs, and is more suitable for continuous fiber prepreg strips or tapes. The essence of the process is the penetration of the thermoplastic resin melt into the interior of the fiber bundles and the replacement of the air between the fiber bundles. The general process flow is shown in figure 1. The fiber tows are pulled by the traction machine and pass through a high-temperature dispersing roller from the release frame to achieve a pre-dispersing effect before entering the impregnation mold and combining with the resin to achieve a cooling effect through the cooling water. The combined material is then cut into prepregs of fixed length by a pelletizer.

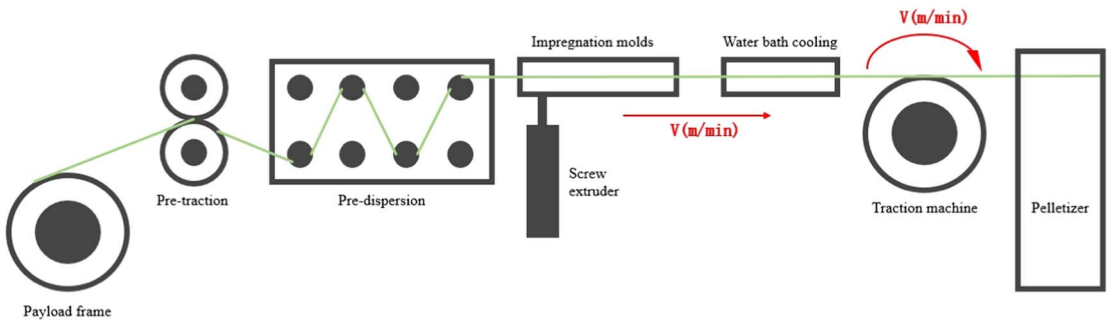

Figure 1. Melt impregnation process flow chart.

In the melt impregnation process, the impregnation process is complicated due to the high viscosity of the resin and the small gap between the fiber monofilaments. The impregnation mold is the essential equipment for the melt impregnation process. By optimizing the structural parameters of the die or increasing the melt impregnation pressure in the die, the degree of impregnation of the prepreg can be improved. Ultrasound is defined as sound waves with a frequency of 2×10^4 to 2×10^9 Hz that interact with the medium during propagation, producing mechanical, cavitation, thermal, and chemical effects [7]. When ultrasonic vibration is applied to the polymer melt, it causes changes in the chemical and physical properties of the polymer and polymer blends due to the physical and chemical effects produced by ultrasonic treatment [8]. In the production process of thermoplastic matrix composites, Lionetto *et al* [9] introduced ultrasonication to the filament winding machine to provide heat and pressure to complete impregnation and consolidation. Through finite element (FE) analysis and simulation, the heat transfer phenomenon occurring during the continuous impregnation and consolidation process was solved. The composite material after ultrasonic treatment has low porosity, and the shear modulus is comparable to the modulus measured by micromechanics. Sinan Liu studied the material removal mechanism in ultrasonic-assisted milling and explored the low-damage machining method with higher precision for CFRTP [10]. By using ultrasonic treatment, Zhong and Isayev [11] prepared PP/CNT composites and found that ultrasonic treatment significantly improved the dispersion of CNTs. All PP is degraded by ultrasonic treatment, especially the PP with high molecular weight. To prepare MWCNT-GFF reinforced composites (MGCs), Zeng *et al* [12] used ultrasonic-assisted impregnation to deposit carboxyl multi-walled carbon nanotubes (MWCNT) onto E glass fiber fabric (GFF). The tensile strength, flexural strength, and interlaminar shear strength of MGC have been significantly improved due to the improved dispersion of MWCNTs and their penetration into the fiber's inner space by ultrasonic treatment.Using ultrasonic consolidation assisted hot pressing sintering technology, Jiao *et al* [13]successfully prepared continuous carbon fiber reinforced Ti/Al_3Ti metal-intermetallic laminate composites. Ultrasonic treatment effectively separated the carbon fiber bundle into single fibers, which were then evenly embedded in the surface of the Al foils layer without any interface macroscopic defect. After ultrasonic treatment, the viscosity of the polymer is reduced, fluidity is improved, compatibility between the two phases of the polymer is significantly improved, and the size of the dispersed phase is reduced, leading to more even distribution of the polymer mixture [14–17]. Köhler [18] *et al* prepared carbon fiber unidirectional polyether ether ketone laminates using ultrasonic welding technology to study the effect of fiber orientation in the layup near the laminate weld on the ultrasonic welding process, thereby optimizing the properties of composite laminates. Oh [19] *et al* investigated the changes of ultrasonic treatment on the microstructure of graphite under different ultrasonic power and treatment time. The graphite-containing silicone composites prepared under the optimal conditions had the best thermal conductivity, and the thermal conductivity of the composites increased with the increase of graphite particle size.

In this paper, we try to introduce ultrasonic devices into the melt impregnation equipment and use the pressurization effect of ultrasonic waves to increase the melt pressure in the impregnation mold to improve the comprehensive performance of BF/PP prepregs. A theoretical model of ultrasonic pressurization is established, and the changes of three parameters, namely, ultrasonic power, frequency, and action distance, with the pressure are experimentally determined. On this basis, orthogonal experiments were designed to prepare online BF/PP ultrasonic-assisted melt-impregnated prepregs. The porosity, fracture rate, and mechanical properties were used as the characterization means to find out the influence laws of the three ultrasonic parameters on the improvement of the impregnation effect of prepregs and the optimal ultrasonic process parameters for the preparation of BF/PP composites were thus determined. It provides theoretical and practical reference and guidance for applying ultrasonic pressurization in the actual continuous production of the melt impregnation. Meanwhile, it also provides new ideas for improving the production quality and efficiency of melt impregnation process.

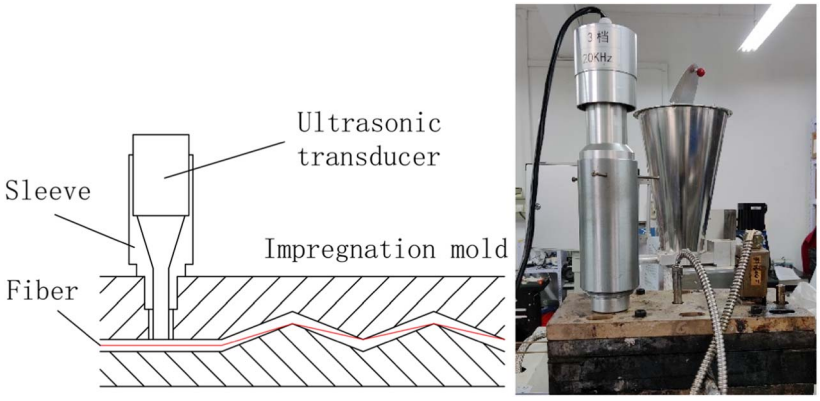

Figure 2. Ultrasonic assisted melt impregnation process device.

Table 1. Experimental materials and related parameters.

Name	Model	Manufacturer	Parameters
BF	BF813–1600B	Sichuan Qian yi	Calibre: 15 μm
PP	Bx3920	Korea SK	Density: 0.91 g cm^{-3} Melt index: 110 g/10 min
Silicone oil	PMX200	/	Viscosity: 1000 cSt Density: 0.98 kg m^{-3}
Compatibilizer	C#	Sinopec	/
Antioxidants	1010	Nanjing Hua li ming	/
Antioxidants	168	Beijing Ji yi	/

Table 2. Experimental equipments.

Name	Model	Manufacturer
Universal Testing Machine	XWW	Chengde Jin Jian Monitoring Instrument Factory
Muffle furnace	SX2–4–10	Wuhan Ya Hua
Injection Molding Machine	MA1200	Ningbo Haitian
Density Tester	PMMD-A	Beijing Guan Mei Precision Electric Instrument
Electronic Balance	MS105DU	METTLER TOLEDO
Ultrasonic controller	Ymnl-1000F	Nanjing Emmanuel Instruments
Precision pressure gauge	YB80A	Suzhou Xuan sheng Instrument
Digital micrometer	32QFF12	Deqing Shengtaixin Electronics

2. Materials and methods

2.1. Raw materials for experiments

The raw materials used in the experiment and their related parameters are shown in table 1.

2.2. Equipment and instruments

Melt impregnation process equipment, Laboratory self-construction, as shown in figures 1 and 2; Equipments used in the experiment and their related information are shown in table 2.

2.3. Theoretical modeling study

Ultrasound, in the process of propagation, will cause alternate compression and elongation of the medium mass, so that the pressure in the medium changes, when the medium by the ultrasound effect, the space at various points generated by the excess pressure, which is the sound pressure. When applying ultrasonic action to the impregnation process, the actual response is so complex that some basic assumptions are made about the model in order to simplify it for ease of calculation:

(1) The melt in the mold is in the region of ultrasonic action, and the acoustic pressure radiation force is the only volumetric force, and is not subject to other external forces such as gravity field and inertia force;

(2) The calculation of the ultrasonic amplitude rod as a series of point vibration sources does not take into account the influence of each other;

(3) The ultrasonic heating effect is neglected;

(4) The mold is always filled with melt, the ultrasonic amplitude rod is always in contact with the melt, and the melt is incompressible;

(5) The distance between the side walls of the mold is much larger than the ultrasonic amplitude rod.

Li [20] derived the calculation formula for parameters including sound pressure, sound intensity, and characteristic impedance of the medium in the ultrasonic field and proposed an ultrasonic-assisted impregnation pressure relationship model with the expression of ultrasonic pressure P*:

$$P^* = \frac{2}{R_z \eta_{a/m}} k_1 W_a \rho_u (Xf^2 + Yf^4) e^{-2(Xf^2+Yf^4)x} \tag{1}$$

where: R_z is the total mechanical resistance of the ultrasonic instrument; W_a(W) is the ultimate mechanical power, $\eta_{a/m}$ is the machine acoustic efficiency, k_1 (m) is the overflow coefficient; x is the ultrasonic action distance; ρ_u (kg/m^3) is ultrasonic treatment medium density; f (Hz) is ultrasound frequency.

The relationship between the total mechanical resistance, machine sound efficiency and ultrasonic mechanical power of the ultrasonic instrument [21]:

$$\frac{1}{R_z \eta_{a/m}} W_a = \frac{1}{2} \omega^2 A^2 \tag{2}$$

where: ω(Hz) is angular frequency of vibration; A(μm) is ultrasonic amplitude.

The phenomenon that the intensity of sound waves decreases with the increase in distance in the medium is called sound attenuation. And the attenuation coefficient α can be calculated:

$$\alpha = Xf^2 + Yf^4 \tag{3}$$

where: Xf^2 represents the medium absorption attenuation coefficient, Yf^4 represents the scattering attenuation coefficient. However, the specific values of parameters X and Y are more difficult to determine, so this chapter will use the following method to determine the attenuation coefficient α.

The variation of ultrasonic pressure with propagation distance [21] x can be expressed:

$$p = 2\alpha E_0 e^{-2\alpha x} \tag{4}$$

where: E_0 is the initial energy of ultrasound.

Taking the natural logarithm of the sound pressure equation yields:

$$\alpha = \frac{1}{2(x_2 - x_1)} \ln\left(\frac{p_1}{p_2}\right) \tag{5}$$

where: p_1, p_2 is the sound pressure at x_1, x_2 from the sound source.

By experimentally measuring the sound pressure at different locations in the melt, the attenuation coefficient can be calculated by substituting the sound pressure and distance data into equation (5). By replacing the attenuation coefficient in equation (1) with equation (5), the optimized ultrasonic pressure expression can be obtained as follows:

$$P^* = \frac{2}{R_z \eta_{a/m}} k_1 W_a \rho_u \alpha e^{-2\alpha x} \tag{6}$$

After obtaining the ultrasonic pressure expression, the theoretical equation for the degree of impregnation and the equation for the fiber breakage rate can be further deduced. The impregnation depth Z_u based on Darcy's Law calculated by ultrasonic action [20] :

$$Z_u = \sqrt{\frac{2KP^*L}{\eta U_0}} \tag{7}$$

Where: K is the penetration rate; L (m) is the distance from the amplitude rod to the first wedge; η(pa • s) is the melt viscosity(the effect of ultrasound is negligible); U_0 (m/s) is the traction speed.

The final theoretical equation (8) for the degree of impregnation D_{imp} after ultrasound action can be obtained as follows:

Table 3. Amplitudes at different ultrasonic powers and frequencies.

f/kHz	P/W	A/μm	f/kHz	P/W	A/μm	f/kHz	P/W	A/μm
20	200	96	25	200	62	28	200	56
	300	107		300	74		300	60
	400	118		400	80		400	65
	500	124		500	87		500	69
	600	130		600	90		600	74

Table 4. Attenuation coefficients of different ultrasonic frequencies.

Ultrasound frequency(f)	20 kHz	25 kHz	28 kHz
Attenuation coefficient(α)	50	75	123

$$D_{imp} = 1 - c_0\left(1 - \frac{Z_u}{H}\right) \tag{8}$$

Where: c_0(%)is the initial porosity of fibers; H (m)is the fiber bundle thickness.

The fibers impregnated under ultrasonic action are subjected to the pressure F_p of the melt and the viscous drag force F_τ', which can be calculated:

$$F_p = \frac{P^*Bl}{N_f} \tag{9}$$

$$F_\tau^{\prime} = \int_c \pi d_0 \tau ds \approx \pi d_0 \tau L \tag{10}$$

Where: B (m)is the fiber bundle spreading width; l (m) is the amplitude rod action distance; N_f is the number of roots of fibers in contact with the melt after ultrasound-assisted impregnation; τ(Pa) is viscous drag stress.

The magnitude of the stress σ_T on the fiber under the action of ultrasound is given:

$$\sigma_T = \frac{4}{\pi {d_0}^2}\left(\frac{F_\tau' \cos\theta + F_p}{\cos\theta} + \frac{F}{N_S}\right) \tag{11}$$

where: N_s is the total number of fibers.

Then the ultrasound-induced fracture rate [20] Br_{ult} is calculated:

$$Br_{ult} = \frac{N_f}{N_s}\left(1 - e^{-\left(\frac{\sigma_T}{\sigma_0}\right)^m}\right) \tag{12}$$

From equations (8) and (11), it can be seen that the ultrasonic action increases the impregnation pressure of the melt, which is beneficiarootl to reduce the porosity of the prepreg. But the increase in pressure also increases the fracture rate, and the theoretical values of the porosity and fracture rate of the prepreg can be derived from equations (8) and (11) after the ultrasonic action.

The power(P) range of the ultrasonic controller used in the experiment is 0 ~ 999 W. Considering the stability of the device's power regulation, control the power rang during the experiment 200 ~ 600 W. The frequency(f) of the transducer consists of three gears, 20 kHz, 25 kHz, and 28 kHz. In different ultrasonic frequency and power, there is a corresponding ultrasonic amplitude(A), these three parameters are ultrasonic controller's own performance parameters.The relevant physical parameters of the ultrasonic device can be obtained as shown in tables 3 and 4.

2.4. Experimental procedure

Variation of internal pressure in silicone oil with different ultrasonic parameters was obtained by installing a precision pressure gauge in the lower part of the vessel containing the silicone oil, and the experimental setup is shown in figure 3.

The meit impregnation process of BF/PP composites is shown in figure 2. The BF/PP prepreg is produced by ultrasonic-assisted melt impregnation process. PP resin contains a double carbon chain, in the impregnation mold by thermal oxygen, mechanical shear, and other effects that are easy to age, resulting in product discoloration and mechanical properties decline [22]. 1010 for the hindered phenolic antioxidants, the processing process to play a stabilizing effect, to prevent the oxidative degradation of polypropylene, often synergistic with the phosphite oxidant 168. Compounding can enhance the effect of antioxidants. Therefore, the formulation of raw materials used for prepreg preparation is: The ratio of PP matrix and compatibilizer to

Figure 3. Ultrasonic viscosity testing device.

Table 5. DOE experimental protocol.

Level	Factors			Response	
	Ultrasound frequency A /kHz	Ultrasonic power B /W	Distance of action C /mm	Porosity %	Fracture rate %
−1	20	300	2	/	/
0	25	400	4	/	/
1	28	500	6	/	/

antioxidant (antioxidant 168 and antioxidant 1010 are compounded in the ratio of 1:1) is 1000:30:3, which is mixed well by adding in a high-speed mixer. The process parameters of the impregnation equipment are set as follows: extruder screw speed is 120 r min^{-1}, impregnation die temperature is 200 °C, fiber dispersion roller temperature is 200 °C, die gap is 2 mm, traction speed is 6 m min^{-1}. The fiber mass fraction in the BF/PP composite produced in this experiment is about 40%, and the prepreg strips are cut into pellets of fixed length 10 mm by the pelletizer.

In order to investigate the effect of three parameters, ultrasonic power, ultrasonic frequency and action distance, on the overall performance of the prepregs after varying the melt pressure and the interaction between the parameters on the results, porosity and fracture rate were taken as the response. The DOE experimental protocol is designed using Design Expert software. Since the three transducer frequencies are 20 kHz, 25 kHz and 28 kHz, the ultrasonic frequency values have been fixed; the ultrasonic power should not be too large to prevent the device from burning out after long working hours. Due to the existence of ultrasonic attenuation, and with the increase of propagation distance attenuation strengthened, as described in the above equation (3), in order to reduce the experimental error caused by this attenuation, the action of the distance should not be too far away, to avoid ultrasonic action in different locations to produce large fluctuation. After comprehensive consideration, the experimental program is shown in table 5.

2.5. Testing and characterization

2.5.1. Porosity

Porosity is used to characterize the impregnation effect of prepreg. The lower the porosity, the better the impregnation effect of prepreg. Porosity is tested according ASTM 2734–09 [23], standard as:

$$\varphi = \frac{\rho_T - \rho_M}{\rho_T} \times 100 \tag{13}$$

$$\rho_T = \frac{m}{m_r/\rho_r + m_f/\rho_f} \tag{14}$$

$$\rho_M = \frac{m}{V} \tag{15}$$

where: φ(%) is the porosity; ρ_T (kg/m^3) is the theoretical density; m (kg) is the prepreg mass; m_r (kg) is the resin mass; m_f (kg) is the fiber mass; ρ_r (kg/m^3) is the resin density; ρ_f (kg/m^3) is the fiber density; ρ_M (kg/m^3) is the measured density; V (m^3) is the measured volume.

Figure 4. Standard sample strips to be tested after experimental injection molding.

2.5.2. Fracture rate

The change in linear density of fiber bundles was used to characterize the fracture rate of the fibers [24]. After measuring the length of each group of specimens, they were calcined in a muffle furnace set at 550 °C for 4 h. The total mass of fibers remaining after cooling at the end of calcination was measured and substituted into equations (16) and (17) to calculate the fracture rate.

$$B_r = \frac{T_0 - T_1}{T_0} \times 100 \tag{16}$$

$$T_1 = \frac{m_f}{L} \tag{17}$$

where: B_r(%) is the fracture rate; T_0(tex) is the initial linear density; T_1(tex) is the residual fiber linear density; L (m) is the total length of the specimen.

2.5.3. Mechanical properties

The prepreg was injected into a standard strip using an injection molding machine, and the mechanical properties were measured after two days. The mechanical properties of the injection molded strips were characterized by the following standards: tensile strength was measured based on GB/T 1447–2005; bending strength was measured based on GB/T 1449–2005; impact strength was measured based on GB/T 1451–2005. The injection molded standard sample strip to be tested is shown in the figure 4.

3. Results and discussion

3.1. Verification and analysis of ultrasound theory

Change the ultrasonic parameters, explore the change rule of ultrasonic pressure, and carry out the comparison and analysis of theoretical and experimental values.

Figures 5 and 6 show the comparison between the theoretical and experimental values of pressure. It can be seen from the figure that the error between the theoretical and experimental values is small, and the trends of change is consistent. The pressure increases with the growth of ultrasonic power and decreases with the growth of action distance. The greater the ultrasonic frequency, the smaller the pressure, and the degree of attenuation also increases with the rise in frequency. Therefore, the melt pressure caused by ultrasonic action can be calculated more accurately by the equation (6).

3.2. Effect of ultrasonic parameters on porosity

The porosity test results in table 6 were analyzed using Design-Expert software, and the transfer function equations obtained by applying the model to fit the response results are as follows:

$$\begin{aligned} \text{Porosity} = {} & 2.70 + 0.099A - 0.18B + 0.32C + 0.12AB + 0.037AC \\ & - 0.037BC + 0.058A^2 + 0.11B^2 + 0.23C^2 \end{aligned} \tag{18}$$

The transfer function model and table 7 can be used to analyze the effects of the three ultrasonic process parameters on porosity and their effect patterns. In the experimental process where the precision of equipment and testing errors cannot be excluded, although the influence of ultrasonic frequency on the porosity results is slightly less significant than the other two, the comparison of the influence degree between the three factors and their influence trend is clear. The influence of process parameters on the porosity is as follows:

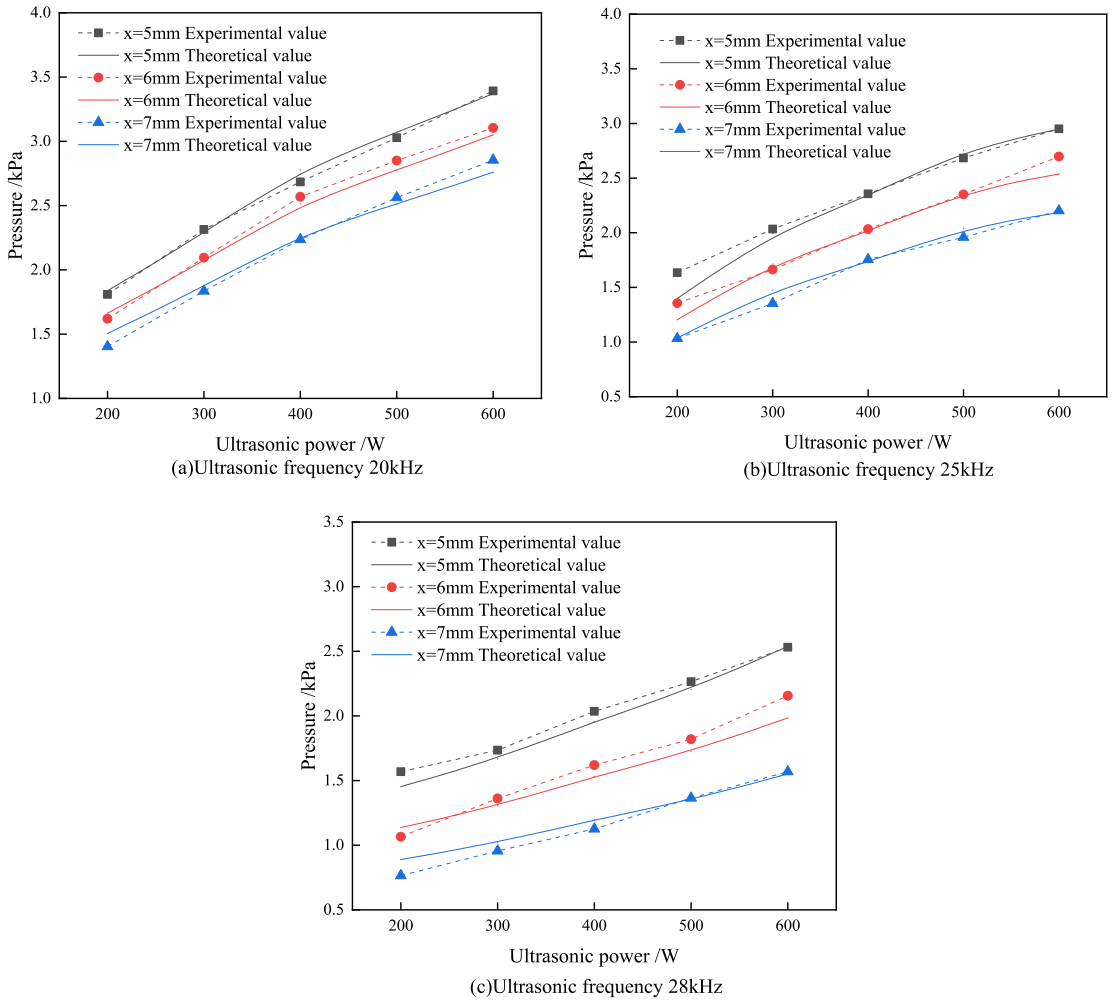

Figure 5. Ultrasonic power and pressure relationship curve.

distance > ultrasonic power > ultrasonic frequency. Porosity increased with increasing distance and ultrasonic frequency (positive correlation) and decreased with increasing ultrasonic power (negative correlation).

As shown in table 7, the quadratic model fits the porosity response well.

From the results of the study in segment 2.3, it is clear that an increase in ultrasonic frequency increases the degree of ultrasonic attenuation and decreases the amplitude, which reduces the ultrasonic action energy and decreases the impregnation pressure [9, 25, 26]. This leads to an increase in the porosity of the prepreg. The change of ultrasonic power directly changes the energy acting on the polymer melt. The higher the ultrasonic power, the higher the local pressure which leading to the easier it is for the resin to infiltrate the fiber bundle. And it increases the degree of impregnation and decreases the porosity. The mechanical effect of ultrasound is severely attenuated in high-viscosity melts, and the greater the action distance, the stronger the attenuation effect. Therefore, as the action distance increases, the ultrasonic energy transferred to the fiber bundle is smaller, thus reducing the impregnation pressure of the resin melt on the fiber bundle, and the impregnation degree of the prepreg is smaller, and the porosity of the prepreg is also larger.

The effect of the interaction of ultrasonic power and distance on the prepreg porosity is shown in figure 7. It can be seen from the figure that the interaction between the two factors is obvious. When the action distance is close, the ultrasonic power has less influence on the porosity, and when the action distance is far, the ultrasonic power has a greater influence on the porosity, and because the dissipation effect is stronger at a distance, the ultrasonic power needs to be increased significantly to achieve a better impregnation effect. Ultrasonic power and action distance can be considered together when adjusting ultrasonic process parameters to achieve the best results.

3.3. Effect of ultrasonic parameters on fracture rate

The the fracture rate test results in table 4 were analyzed using Design-Expert software, and the transfer function equations obtained by applying the model to fit the response results are as follows:

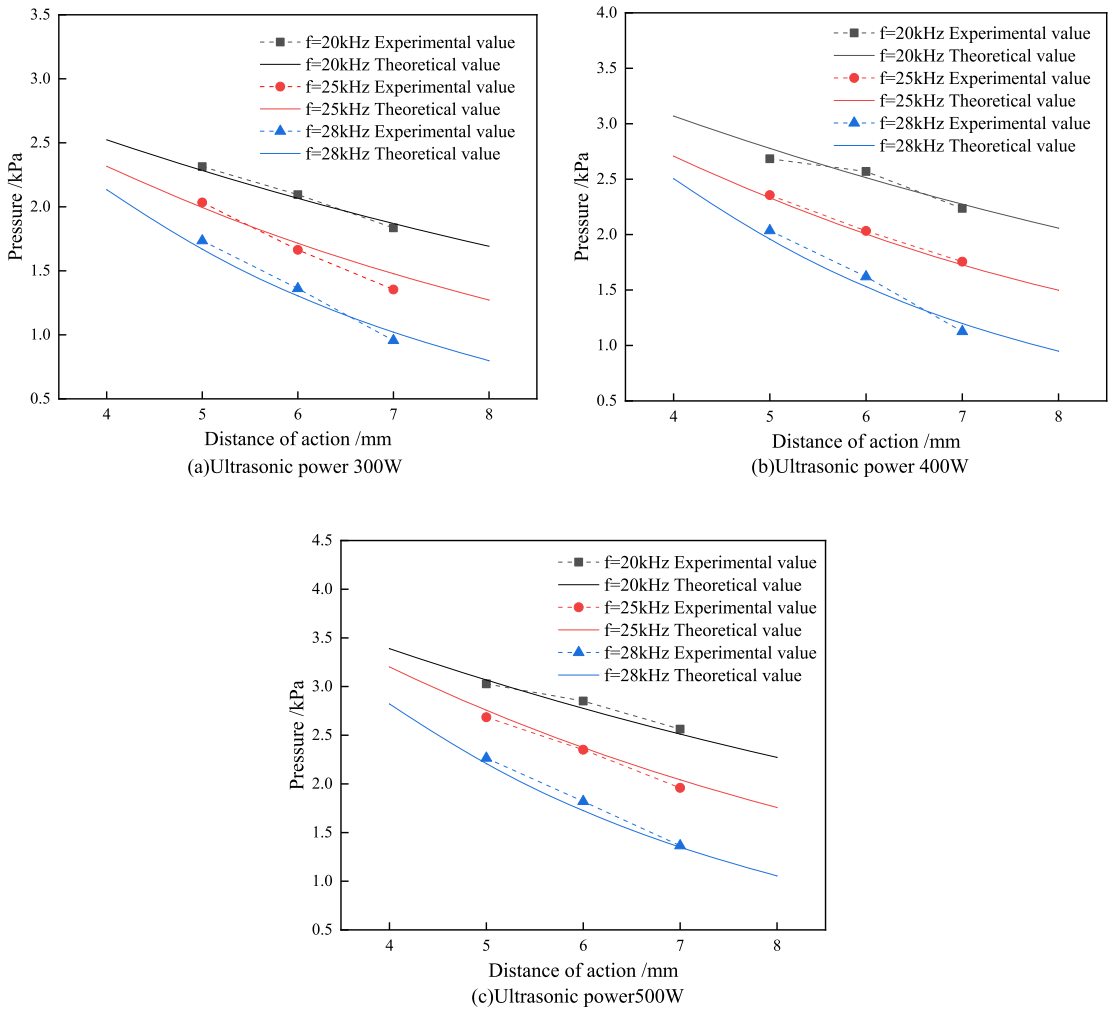

Figure 6. Ultrasonic pressure and distance of action relationship curve.

Table 6. DOE experimental results.

Serial number	Ultrasound frequency A kHz	Ultrasonic power B w	Distance of action C mm	Porosity %	Fracture rate %
1	25.00	400.00	4.00	2.75	3.86
2	25.00	500.00	2.00	2.73	5.58
3	20.00	400.00	2.00	2.51	4.72
4	25.00	300.00	6.00	3.48	3.13
5	25.00	300.00	2.00	2.81	3.66
6	25.00	400.00	4.00	2.67	3.96
7	20.00	500.00	4.00	2.49	4.72
8	20.00	400.00	6.00	3.12	3.11
9	25.00	400.00	4.00	2.79	3.92
10	28.00	300.00	4.00	3.04	3.53
11	28.00	400.00	6.00	3.55	2.94
12	28.00	500.00	4.00	2.75	4.49
13	25.00	400.00	4.00	2.64	3.69
14	20.00	300.00	4.00	3.19	3.54
15	28.00	400.00	2.00	2.76	4.65
16	25.00	500.00	6.00	3.25	3.63
17	25.00	400.00	4.00	2.78	3.77

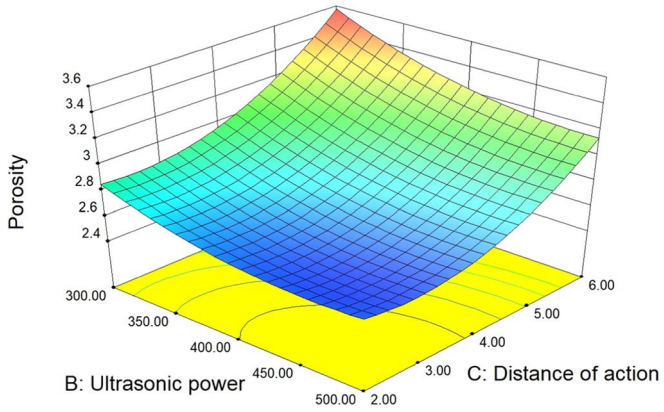

Figure 7. The interactive effect of ultrasonic power and action distance on porosity.

Table 7. ANOVA analysis of porosity.

/	Sum of squares	df	Mean square	F Value	p-value Prob>F	Significance
Source Model	1.50	9	0.17	10.86	0.0024	significant
A- Ultrasound frequency	0.078	1	0.078	5.10	0.0584	
B- Ultrasonic power	0.24	1	0.24	16.00	0.0052	
C- Distance of action	0.79	1	0.79	51.70	0.0002	
AB	0.059	1	0.059	3.88	0.0894	
AC	5.731E-003	1	5.731E-003	0.37	0.5598	
BC	5.625E-003	1	5.625E-003	0.37	0.5633	
A^2	0.012	1	0.012	0.78	0.4057	
B^2	0.053	1	0.053	3.45	0.1054	
C^2	0.22	1	0.22	14.50	0.0066	
Residual	0.11	7	0.015			
Lack of Fit	0.089	3	0.030	6.54	0.0506	not significant
Pure Error	0.018	4	4.530E-003			
Cor Total	1.60	16				

Table 8. ANOVA analysis of fracture rate.

/	Sum of squares	df	Mean square	F Value	p-value	Significance
Source Model	7.35	6	1.23	39.82	< 0.0001	significant
A- Ultrasound frequency	0.035	1	0.035	1.12	0.3142	
B- Ultrasonic power	2.57	1	2.57	83.62	< 0.0001	
C- Distance of action	4.08	1	4.08	132.71	< 0.0001	
AB	8.297E-003	1	8.297E-003	0.27	0.6148	
AC	6.061E-006	1	6.061E-006	1.970E-004	0.9891	
BC	0.50	1	0.50	16.38	0.0023	
Residual	0.31	10	0.031			
Lack of Fit	0.26	6	0.043	3.55	0.1201	not significant
Pure Error	0.049	4	0.012			
Cor Total	7.66	16				

$$\text{Fracture rate} = 3.94 - 0.065A + 0.58B - 0.73C - 0.045AB - 0.001212AC - 0.35BC \quad (19)$$

The transfer function model can be used to analyze the effects of three ultrasonic process parameters on the fracture rate and their action patterns. In order to harvest the highly fitted fracture rate response model, the 2FI model was used for fitting, and the results are shown in table 8. The effects of the three factors were as follows: distance > ultrasonic power > ultrasonic frequency, which was consistent with the effects of porosity. The

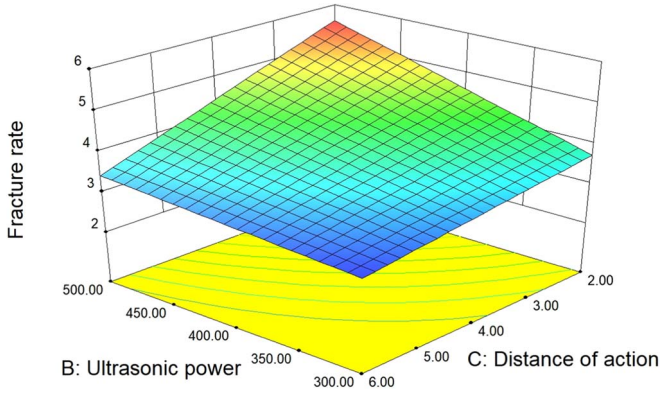

Figure 8. The interactive effect of ultrasonic power and action distance on fracture rate.

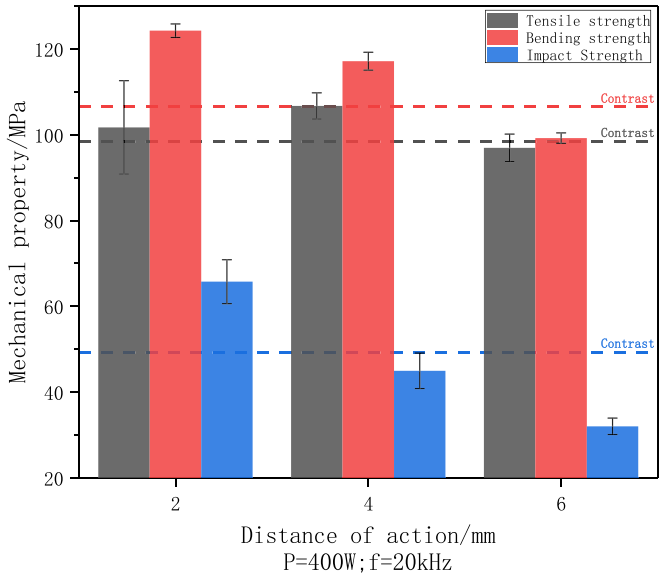

Figure 9. Relationship between action distance and mechanical properties.

model shows that the ultrasonic frequency is less significant than the other two factors, but the influence of the three factors has the same trend. The fracture rate decreases (negative correlation) with the increase of acting distance and ultrasonic frequency and increases (positive correlation) with the increase of ultrasonic power.

From the experimental results, it can be seen that the increase in ultrasound frequency increases the degree of ultrasound attenuation and decreases the ultrasonic energy and impregnation pressure, which leads to the decrease in the fracture rate of the fiber bundle [20]. The higher the ultrasonic power, the stronger the vibration effect of ultrasonic action transferred to the resin melt, the greater the local pressure between the resin and fiber bundle. At the same time, the pressure of the resin acting on the fiber bundle will also increase, which will promote the resin melt impregnation. Every coin has two sides, it also increases the stress on the fiber, so it will also lead to an increase in the fiber bundle fracture rate. According to the model of fiber bundle fracture probability distribution, the smaller the stress on the fiber bundle, the lower the fiber bundle fracture rate.

The effect of the interaction between ultrasonic power and distance on the fracture rate of prepreg in the experiment is shown in figure 8. The interaction between the two factors is obvious, and it can be seen that when the action distance is closer, the ultrasonic power has a high degree of influence on the fracture rate of fiber bundles; when the action distance is farther, the ultrasonic power has a lower degree of influence on the fracture rate. Therefore, it is necessary to consider ultrasonic power and action distance when adjusting ultrasonic process parameters in order to achieve the best results.

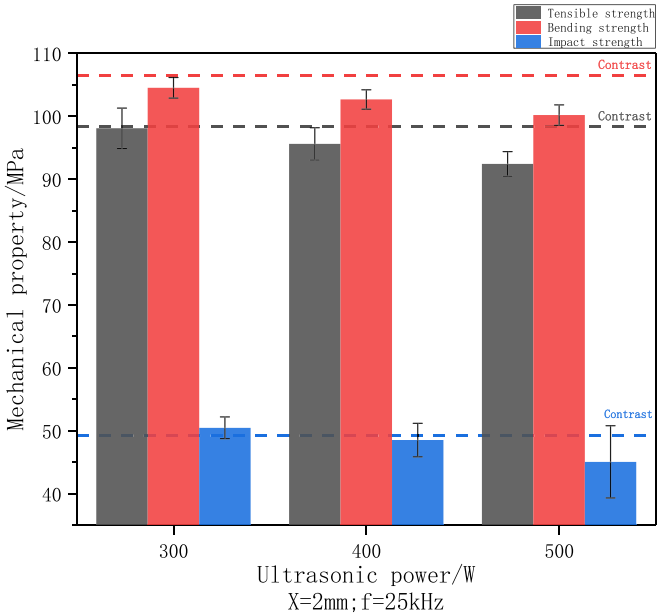

Figure 10. The relationship between ultrasonic power and mechanical properties.

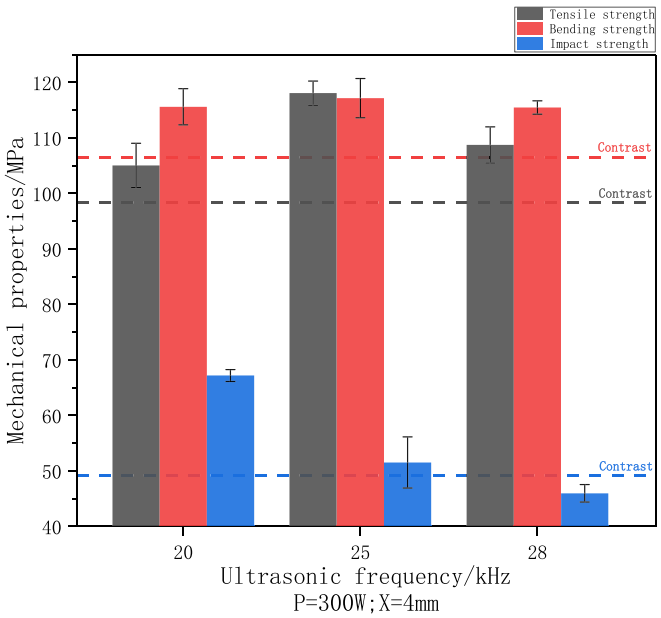

Figure 11. The relationship between ultrasonic frequency and mechanical properties.

3.4. Effect of ultrasonic parameters on mechanical properties

The mechanical properties of the prepreg under different ultrasonic process parameters were measured, and the results are shown in figures 9 to 11. It can be seen that the increase in the action distance can somewhat reduce the porosity and increase the fiber fracture rate, in such a case, the bending strength and impact strength are enhanced. Focusing on the tensile strength, the best tensile strength is achieved when the action distance is 4 mm under the interaction of porosity and fracture rate. Compared with the porosity, the increase in ultrasonic power mostly increases the fracture rate of fibers, resulting in a decrease in mechanical properties. The increase of ultrasonic frequency causes the decrease of fracture rate and the increase of porosity, and the two tend to balance when the frequency reaches 25kHZ. During the change, the tensile strength and bending strength increase and then decrease, and the two reach the best value when the frequency reaches 25kHZ. However, the impact strength decreases due to the increase of porosity.

The production of prepregs using the melt impregnation process requires an optimal balance between porosity and fracture rate. A low porosity reduces defects and improves the mechanical properties of the product produced by the subsequent molding process. A high fracture rate can lead to unstable fiber content of the prepreg, while broken fibers can clog the mold opening die, interrupting continuous production and reducing productivity. The theoretical and experimental analyses in section 3 show that ultrasonic action causes changes in melt pressure, which will directly affect the porosity and fracture rate of the prepreg [11, 14, 15, 20, 27]. The increase in ultrasonic power, the decrease in ultrasonic frequency, and the decrease in the action distance will increase the melt pressure, which will lead to a decrease in porosity and an increase in fracture rate. Therefore, it is not possible to achieve the goal of reducing porosity while maintaining a low fracture rate, and a comprehensive analysis of the prepreg porosity, fracture rate, and final mechanical properties is required.

Combined with the analysis of Design Expert software [28, 29], the optimum values were achieved within the experimentally set process parameters of 25 kHz ultrasonic frequency, 300 W ultrasonic power, and 4 mm action distance. In this case the porosity was 2.99%, fracture rate was 3.36%, tensile strength was 108.73 MPa, bending strength was 116.81 MPa, and impact strength was The porosity was 5.68%, the fracture rate was 2.79%, the tensile strength was 98.36 $kJ{\cdot}m^{-2}$, the bending strength was 106.52 MPa, and the impact strength was 49.22 $kJ{\cdot}m^{-2}$ without ultrasonic impregnation. Tensile strength, flexural strength, and impact strength were respectively increased by 10.5%, 9.7%, and 4.8%. Porosity decreased by 47.4% and fracture rate increased by 20.4%. The reduction of porosity of prepreg after ultrasonic treatment was greater than the increase in fracture rate, so the ultrasonic-assisted impregnation was beneficial to improving the impregnation quality and the performance of the composites.

4. Conclusion

(1) Combined with the optimized ultrasonic building model, the experimental and theoretical joint results of ultrasonic pressure building are derived: the higher the ultrasonic power, the lower the frequency, and the closer the action distance, the higher the ultrasonic pressure.

(2) The DOE orthogonal test shows that increasing the ultrasonic power, decreasing the action distance and ultrasonic frequency can reduce the porosity, and decreasing the ultrasonic power, increasing the action distance and ultrasonic frequency can reduce the fracture rate. From the fitted transfer function model, it can also be seen that the action distance has the greatest influence on the porosity and fracture rate, the ultrasonic frequency has the least influence on the porosity and fracture rate, and the interaction between the ultrasonic power and the action distance has obvious influence on the porosity and fracture rate.

(3) The best ultrasonic process parameters were optimized by software: ultrasonic frequency was 25 kHz, ultrasonic power was 300 W, and the action distance was 4 mm, at which the porosity was 2.99%, the fracture rate was 3.36%, and the tensile strength, bending strength and impact strength were 108.73 MPa, 116.81 MPa and 51.59 $kJ{\cdot}m^{-2}$, respectively.

Data availability statement

The data cannot be made publicly available upon publication because they are owned by a third party and the terms of use prevent public distribution. The data that support the findings of this study are available upon reasonable request from the authors.

ORCID iDs

Yang Yu https://orcid.org/0000-0001-9592-8191

References

[1] Dandan Z, Yaoning S and Ya W 2017 Failure behavior and damage mechanism of multiaxial glas-s fiber reinforced resin matrix composites *Acta Materiae Compositae Sinica.* **34** 381–8
[2] Vaidya U K and Chawla K K 2008 Processing of fibre reinforced thermoplastic composites *Int. Mater. Rev.* **53** 185–218
[3] Peng L 2009 *Progress in Applications of Long Fiber Reinforced Thermoplastics in Automotive Parts* (China Plastics)
[4] Gupta M, Raj R and Sahu A K 2022 Mechanical properties of high strength concrete incorporating chopped basalt fibers: experimental and analytical study *Mater. Res. Express* **9** 125305
[5] Wang X *et al* 2019 Static and fatigue behavior of basalt fiber-reinforced thermoplastic epoxy composites *J. Compos. Mater.* **54** 2389–98
[6] Li Y-F *et al* 2024 Effect of the sizing removal methods of fiber surface on the mechanical performance of basalt fiber-reinforced concrete *Fibers.* **12** 10

[7] Ganjian E et al 2018 Application of power ultrasound to cementitious materials: advances, issues and perspectives *Mater. Des.* **160** 503–13
[8] Zhao Y et al 2018 Ultrasonic processing of MWCNT nanopaper reinforced polymeric nanocomposites *Polymer* **156** 85–94
[9] Lionetto F et al 2016 Modeling of continuous ultrasonic impregnation and consolidation of thermoplastic matrix composites *Composites Part A: Applied Science and Manufacturing* **82** 119–29
[10] Liu S et al 2023 Investigating the material removal mechanism and cutting performance in ultrasonic vibration-assisted milling of carbon fibre reinforced thermoplastic *Mater. Res. Express* **10** 095603
[11] Zhong J and Isayev A I 2016 Ultrasonically assisted compounding of CNT with polypropylenes of different molecular weights *Polymer* **107** 130–46
[12] Zeng S et al 2018 Effect of ultrasonic-assisted impregnation parameters on the preparation and interfacial properties of MWCNT/glass-fiber reinforced composites *e-Polymers* **18** 35–47
[13] Jiao F et al 2019 Continuous carbon fiber reinforced Ti/Al3Ti metal-intermetallic laminate (MIL) composites fabricated using ultrasonic consolidation assisted hot pressing sintering *Materials Science and Engineering* A **765** 138255
[14] Gao X et al 2017 Influence of processing parameters during ultrasound assisted extrusion on the properties of polycarbonate/carbon nanotubes composites *Compos. Sci. Technol.* **144** 125–38
[15] Gao X, Isayev A I and Yi C 2016 Ultrasonic treatment of polycarbonate/carbon nanotubes composites *Polymer* **84** 209–22
[16] Zhong J and Isayev A I 2014 Properties of polyetherimide/graphite composites prepared using ultrasonic twin-screw extrusion *J. Appl. Polym. Sci.* **132** 41397
[17] Mata-Padilla J M et al 2014 Structural and morphological studies on the deformation behavior of polypropylene/multi-walled carbon nanotubes nanocomposites prepared through ultrasound-assisted melt extrusion process *J. Polym. Sci., Part B: Polym. Phys.* **53** 475–91
[18] Köhler F et al 2021 Static ultrasonic welding of carbon fibre unidirectional thermoplastic materials and the influence of heat generation and heat transfer *J. Compos. Mater.* **55** 2087–102
[19] Oh W, Bae J-S and Moon H-S 2021 Thermal conduction characteristics of silicone composites including ultrasonic-treated graphite *J. Compos. Mater.* **56** 619–26
[20] Li R 2020 Study on the preparation process of ultrasound-assisted fiber-reinforced polypropylene composites *Master thesis* Beijing University of Chemical Technology, Beijing, China
[21] Enhua X and Xiaoqian L 2009 Acoustic streaming phenomenon during ultrasonic sonication on melt *University of Science and Technology Beijing* **31** 1425–9
[22] Xi-Hui G et al 2024 Effect of different antioxidant systems on processing stability of polypropylene *Plastics Science and Technology* **52** 36–9
[23] ASTM D2734–09 2009 International Standard test methods for porosity of reinforced plastics *ASTM D2734–09* 1–3
[24] Cong Z et al 2015 Fiber fracture mechanism in proc-ess of thermoplastic resin continuous impregnation and experiments *Acta Materiae Compositae Sinica.* **32** 983–8
[25] Ligao D et al 2008 Advances in changes mechanism of polymer in ultrasonic field *Food Science* **29** 744–7
[26] Chen G, Guo S and Li H 2002 Ultrasonic improvement of rheological behavior of polystyrene *J. Appl. Polym. Sci.* **84** 2451–60
[27] Yang M et al 2017 Effects of ultrasonic treatment on the transesterification of PC/PMMA blends *Polymer Engineering & Science* **58** 1508–15
[28] Yu Y et al 2023 Corrosion and coating defect assessment of coal handling and preparation plants (CHPP) using an ensemble of deep convolutional neural networks and decision-level data fusion *Neural Computing and Applications* **35** 18697–718
[29] Yu Y et al 2023 Compressive strength evaluation of cement-based materials in sulphate environment using optimized deep learning technology *Developments in the Built Environment* **16** 100298